Phase equilibria of a square-well monomer-dimer mixture: Gibbs ensemble computer simulation and statistical associating fluid theory for potentials of variable range

Lowri A. Davies, Alejandro Gil-Villegas, and George Jackson
Department of Chemistry, University of Sheffield, Sheffield S3 7HF, United Kingdom

Sofía Calero and Santiago Lago
Departamento de Química Fundamental e Industrial, Facultad de Ciencias, Universidad de la Coruña, 15071 Coruña, Spain

(Received 4 August 1997)

The vapor-liquid equilibria of a monomer-dimer square-well mixture is examined. The square-well segments all have equal diameter, well depth, and range ($\lambda = 1.5$); the dimers are formed from two tangentially bonded monomers. The phase behavior in this system is thus governed by the difference in molecular length of the two components. Pressure-composition slices of the phase diagram are obtained from Gibbs ensemble simulation of the mixture for a wide range of temperatures, including both subcritical and supercritical states. A small negative deviation from ideality is observed. The simulation data are used to determine the vapor-liquid critical line of the mixture. Additionally, we extrapolate the mixture data to obtain an estimate of the pure component phase equilibria. The resulting values for the coexistence envelope are in good agreement with existing data, and new vapor pressures of the square-well dimer are reported. The vapor-liquid equilibria data are used to establish the adequacy of the statistical associating fluid theory for potentials of variable range. The theory is found to give an excellent representation of the phase behavior of both the pure components and of the mixture. [S1063-651X(98)12302-4]

PACS number(s): 64.70.Fx

I. INTRODUCTION

The system of interest in this paper is a monomer-dimer binary mixture. This is an important prototype system which allows one to quantify the effect of chain length on fluid phase equilibria. Although the phase equilibria of such systems have been studied experimentally (e.g., mixtures of homologous series such as alkanes, perfluoroalkanes, dimethysiloxanes, etc.), the complexity of the real intermolecular interactions makes it difficult to establish the precise effect of molecular extension. The effect of chain length on the vapor-liquid equilibria for a square-well monomer-dimer mixture is examined here using both a theoretical and a simulation approach. The dimer is formed from two tangentially bonded square-well monomers so that the segments comprising the monomers and dimers have the same range and strength of interaction. Particular attention is paid to the vapor-liquid critical behavior.

The Gibbs ensemble Monte Carlo (GEMC) simulation technique is widely used in the determination of the fluid-phase equilibria of mixtures [1–3]. The method has been used to describe the vapor-liquid coexistence for mixtures of hard spheres and square wells [4], and the liquid-liquid coexistence of symmetrical square-well mixtures in which there are no unlike interactions [5,4,6]. Here, we report GEMC simulation results for a binary mixture of monomers and dimers with segments interacting by means of square-well potentials of range $\lambda = 1.5$, as a natural extension to the previous studies. This enables us to focus on the effect of increasing the chain length of one component on the phase diagram of the mixture. Simultaneously, the simulation data obtained for the phase equilibria of the mixture are used to test the adequacy of the recently developed statistical associating fluid theory for potentials of variable range (SAFT-VR) [7,8].

The statistical associating fluid theory (SAFT) [9,10], which is based on the thermodynamic perturbation theory of Wertheim [11–16], is now widely accepted as being one of the most powerful predictive tools in the description of the phase equilibria for both pure fluids and mixtures (see [7] and references therein). The SAFT equation of state describes the thermodynamic properties of associating chain molecules formed from spherical segments. Although the original SAFT free energy is based on the hard-sphere reference structure, it has now been extended to include an accurate representation of the monomer structure [17–21], to include higher-body interactions in its dimer versions [22,23], to deal with double bonding [24], ring formation [25–28], and bond cooperativity [29], and to describe the isotropic-nematic phase transition [30,31]. Quite recently, the theory has been formulated to include a description of a chain of segments interaction through attractive [7,8] and repulsive [32] potentials of variable range (SAFT-VR); this is a particularly important extension of the original SAFT approach as it enables a description of nonconformal properties. The SAFT-VR formalism is based on the Barker and Henderson perturbation theory [33–35] with a compact and accurate expression for the mean-attractive energy. This is obtained using the mean-value theorem and results in an equation of state which can be applied to systems of chain molecules with different interaction potentials of variable range, where the dispersive interactions are treated at a level beyond that of the mean-field (van der Waals) approach. An important advantage of molecular-based theories such as SAFT is that each of the individual contributions to the equation of state can be compared directly with computer simulation data.

II. GIBBS ENSEMBLE MONTE CARLO SIMULATIONS

Since its introduction 10 years ago by Panagiotopoulos [1,2], the GEMC technique has become the most commonly used direct simulation technique for the determination of phase equilibria in fluid systems [36,3]. The isothermal-isobaric (NPT) version of GEMC, as applied to mixtures, consists of a separate simulation in two distinct regions a and b, with volumes V^a and V^b, containing N^a and N^b particles, such that $V=V^a+V^b$ and $N=N^a+N^b$. The two regions are in thermodynamic equilibrium, but not in physical contact. In order for two or more phases in a mixture to be in equilibrium with one another, the pressures, temperatures, and chemical potentials of each component must be equal in the coexisting a and b phases:

$$T^a=T^b, \qquad P^a=P^b, \qquad \mu_i^a=\mu_i^b. \tag{1}$$

Three distinct Monte Carlo moves are performed in the GEMC technique in order to satisfy these conditions: particle displacements and reorientations (see Ref. [37]) within either subsystem to maintain equality of temperature; volume changes of either subsystem to maintain equality of pressure; and particle interchanges between the two subsystems to maintain equality of chemical potential. As a consequence, the energy E^j, volume V^j, and composition $x_i^j=N_i^j/N^j$ of particles of type i in subsystem j will vary during the course of the simulation. We use the particle transfer algorithm originally proposed for mixtures by Panagiotopoulos *et al.* [2], although other algorithms can be used [38]. The acceptance criterion for each of these moves in the NPT Gibbs ensemble is governed by the pseudo-Boltzmann probability distribution [2]:

$$\mathcal{P}^{\text{Gibbs}}=\exp\left[\ln\left(\frac{N_1!}{N_1^a!N_1^b!}\right)+\ln\left(\frac{N_2!}{N_2^a!N_2^b!}\right)+N^a\ln V^a+N^b\ln V^b-\frac{PV^a}{kT}-\frac{PV^b}{kT}-\frac{E^a(N^a)}{kT}-\frac{E^b(N^b)}{kT}\right]. \tag{2}$$

The reader is referred to the original papers for details.

The model mixture we consider is a binary mixture of $N=N_1+N_2$ particles, N_1 monomers and N_2 dimers, at a constant temperature T and a constant pressure P. The monomers are square-well particles of diameter σ with an attractive well of depth ε and range $\lambda\sigma=1.5\sigma$. The dimers are formed by tangentially bonding two of the square-well monomers so that the bond length is σ; the strength and range of the square-well interaction are therefore the same in the monomer and dimer particles. Computer simulations for the vapor-liquid equilibria have already been reported for the pure monomer [39,40,6] and the pure dimer [41] systems.

Simulations are performed in cubic boxes. The particles in the vapor subsystem are initially arranged on a face-centered-cubic (fcc) lattice, while the higher density liquid configurations are obtained by compressing a single subsystem with a standard NPT Monte Carlo technique [42,43]. The usual periodic boundary conditions (PBC) and minimum image convention (MIC) are used [43]. Initial guesses for the coexisting densities and compositions at each pressure and temperature state point are made by using the corresponding SAFT-VR solutions (see the following section); one must always ensure that the overall composition of the system lies somewhere between the compositions of the two coexisting phases. The chemical potential was determined with the Widom test particle technique [44] as adapted to the GEMC approach [45], in order to ensure that phase equilibria is achieved. The use of the NPT version of the Gibbs ensemble technique yields constant pressure slices of the phase diagram of the mixture. One simulation cycle consists of N displacements and reorientations in each box, one volume change for either box, and a specific number of particle interchanges. The maximum displacement and volume change are adjusted to give an acceptance ratio of between 30% and 40%, and the number of insertions is controlled so that between 1% and 3% of particles are interchanged each cycle. The majority of the simulations are performed with systems of $N=512$ particles, but it is necessary to use $N=1728$ particles to get closer to the critical line of the mixture. An initial simulation of 50 000 cycles is performed to equilibrate the subsystems, before averaging for between 100 000 and 250 000 cycles.

III. SAFT-VR EQUATION OF STATE

The SAFT-VR equation of state for a mixture of associating chain molecules is written in terms of four separate contributions to the Helmholtz free energy, A [7,8],

$$\frac{A}{NkT}=\frac{A^{\text{ideal}}}{NkT}+\frac{A^{\text{mono}}}{NkT}+\frac{A^{\text{chain}}}{NkT}+\frac{A^{\text{assoc}}}{NkT}, \tag{3}$$

where N is the number of chain molecules in the mixture, k is the Boltzmann constant, and T is the temperature. In this equation, A^{ideal} is the ideal free energy, A^{mono} is the residual free energy due to the monomer segments, A^{chain} is the contribution due to the formation of chains of monomers, and A^{assoc} is the term that describes the contribution to the free energy due to intermolecular association. In this paper we focus on systems interacting with a square-well potential:

$$u_{ij}(r_{ij})=\begin{cases}+\infty & \text{if } r_{ij}<\sigma_{ij},\\ -\varepsilon_{ij} & \text{if } \sigma_{ij}\leqslant r_{ij}<\lambda_{ij}\sigma_{ij},\\ 0 & \text{if } r_{ij}\geqslant\lambda_{ij}\sigma_{ij},\end{cases} \tag{4}$$

where r_{ij} is the distance between two particles. The contact distance is σ_{ij} and the parameters λ_{ij} and ε_{ij} are the range and depth of the potential well for the i-j interaction, respectively. For our particular system $\sigma=\sigma_{11}=\sigma_{12}=\sigma_{22}$, $\varepsilon=\varepsilon_{11}=\varepsilon_{12}=\varepsilon_{22}$, and $\lambda=\lambda_{11}=\lambda_{12}=\lambda_{22}$. We will present the general SAFT-VR expressions for the free energy for each contribution [7,8] together with the specific ones for our monomer-dimer system.

The free energy of the ideal n-component mixture is given by [46]

$$\frac{A^{\text{ideal}}}{NkT}=\sum_{i=1}^{n}x_i\ln\rho_i\Lambda_i^3-1=x_1\ln\rho_1\Lambda_1^3+x_2\ln\rho_2\Lambda_2^3-1, \tag{5}$$

where $x_i = N_i/N$ is the mole fraction, $\rho_i = N_i/V$ is the number density, and Λ_i is the thermal de Broglie wavelength of species i.

The monomer free energy is

$$\frac{A^{\text{mono}}}{NkT} = \left(\sum_{i=1}^{n} x_i m_i\right) \frac{A^M}{N_s kT} = \left(\sum_{i=1}^{n} x_i m_i\right) a^M = (x_1 + 2x_2) a^M, \tag{6}$$

where m_i is the number of spherical segments in each chain i, $m=1$ for the monomer (component 1), $m=2$ for the dimer (component 2) and N_S is the total number of segments. The monomer free energy per segment of the mixture $a^M = A/(N_s kT)$ is obtained from the Barker and Henderson high-temperature expansion [33–35]:

$$a^M = a^{\text{HS}} + \beta a_1 + \beta^2 a_2, \tag{7}$$

where a^{HS} is the free energy for a mixture of hard spheres, $\beta = 1/kT$, and a_1 and a_2 are the first two perturbation terms associated with the attractive energy.

The free energy of the reference hard-sphere mixture is obtained from the expression of Boublík [47] and Mansoori *et al.* [48]:

$$a^{\text{HS}} = \frac{6}{\pi\rho_s}\left[\left(\frac{\zeta_2^3}{\zeta_3^2} - \zeta_0\right)\ln(1-\zeta_3) + \frac{3\zeta_1\zeta_2}{1-\zeta_3} + \frac{\zeta_2^3}{\zeta_3(1-\zeta_3)^2}\right]. \tag{8}$$

In this expression, $\rho_s = N_s/V$ is the number density of the mixture in terms of the number of spherical segments. Note that $\rho_s = \rho(\Sigma_{i=1}^{n} x_i m_i)$, where ρ is the total number density of the mixture. The reduced densities ζ_l are defined as

$$\zeta_l = \frac{\pi}{6}\rho_s\left[\sum_{i=1}^{n} x_{s,i}(\sigma_i)^l\right], \tag{9}$$

where σ_i is the diameter of spherical segments of chain i, and $x_{s,i}$ is the mole fraction of segments of type i in the mixture, given by

$$x_{s,i} = \frac{m_i x_i}{\sum_{k=1}^{n} m_k x_k}. \tag{10}$$

For the monomers we have

$$x_{s,1} = \frac{x_1}{x_1 + 2x_2} \tag{11}$$

and for the dimers,

$$x_{s,2} = \frac{2x_2}{x_1 + 2x_2}. \tag{12}$$

The overall packing fraction of the mixture is given by ζ_3, which is equivalent to $\eta = \pi\rho\sigma^3/6$ for the pure component. In our case since $\sigma = \sigma_1 = \sigma_2$ the free energy of the reference hard-sphere mixture reduces to the Carnahan and Starling expression [49,46]

$$a^{\text{HS}} = \frac{4\eta - 3\eta^2}{(1-\eta)^2}. \tag{13}$$

The mean-attractive energy a_1 in the perturbation expansion is given by

$$a_1 = \sum_{i=1}^{n}\sum_{j=1}^{n} x_{s,i} x_{s,j} a_1^{ij}, \tag{14}$$

where

$$a_1^{ij} = -2\pi\rho_s\varepsilon_{ij}\int_{\sigma_{ij}}^{\infty} r_{ij}^2 g_{ij}^{\text{HS}}(r_{ij};\zeta_3)\,dr_{ij}, \tag{15}$$

and g_{ij}^{HS} is the radial distribution function for a mixture of hard spheres. The integral is transformed by applying the mean-value theorem [7], which gives an expression for a_1 in terms of the contact value of g_{ij}^{HS}:

$$a_1 = -\rho_s\sum_{i=1}^{n}\sum_{j=1}^{n} x_{s,i} x_{s,j}\alpha_{ij}^{\text{VDW}} g_{ij}^{\text{HS}}[\sigma_{ij};\zeta_3^{\text{eff}}], \tag{16}$$

where

$$\alpha_{ij}^{\text{VDW}} = 2\pi\varepsilon_{ij}\sigma_{ij}^3(\lambda_{ij}^3 - 1)/3 \tag{17}$$

is the van der Waals attractive constant for the i-j interaction. The contact value of the radial distribution function for the hard-sphere reference system, $g_{ij}^{\text{HS}}[\sigma_{ij};\zeta_3^{\text{eff}}]$, is evaluated at an effective packing fraction ζ^{eff}, given by the expression of Boublík [47] and Mansoori *et al.* [48],

$$g_{ij}^{\text{HS}}[\sigma_{ij};\zeta_3^{\text{eff}}] = \frac{1}{1-\zeta_3^{\text{eff}}} + 3\frac{\sigma_{ii}\sigma_{jj}}{\sigma_{ii}+\sigma_{jj}}\frac{\zeta_2^{\text{eff}}}{(1-\zeta_3^{\text{eff}})^2} + 2\left(\frac{\sigma_{ii}\sigma_{jj}}{\sigma_{ii}+\sigma_{jj}}\right)^2\frac{\zeta_2^{\text{eff}^2}}{(1-\zeta_3^{\text{eff}})^3}. \tag{18}$$

For our system the mean-attractive energy reduces to

$$a_1 = -\rho_s\alpha^{\text{VDW}} g^{\text{HS}}[\sigma;\eta^{\text{eff}}], \tag{19}$$

where

$$\alpha^{\text{VDW}} = 2\pi\varepsilon\sigma^3(\lambda^3 - 1)/3 \tag{20}$$

and $g_{ij}^{\text{HS}}[\sigma_{ij};\zeta_3^{\text{eff}}]$ becomes the Carnahan and Starling expression [49,46],

$$g^{\text{HS}}[\sigma;\eta^{\text{eff}}] = \frac{1-\eta^{\text{eff}}/2}{(1-\eta^{\text{eff}})^3}, \tag{21}$$

with $\eta^{\text{eff}} = \zeta_3^{\text{eff}}$. The parametrization for η^{eff} obtained for the pure square-well fluid [7] is used:

$$\eta^{\text{eff}}(\eta,\lambda) = c_1(\lambda)\eta + c_2(\lambda)\eta^2 + c_3(\lambda)\eta^3, \tag{22}$$

where the coefficients c_1, c_2, and c_3 are given by

$$\begin{pmatrix} c_1 \\ c_2 \\ c_3 \end{pmatrix} = \begin{pmatrix} 2.258\,55 & -1.503\,49 & 0.249\,434 \\ -0.669\,270 & 1.400\,49 & -0.827\,739 \\ 10.1576 & -15.0427 & 5.308\,27 \end{pmatrix} \begin{pmatrix} 1 \\ \lambda \\ \lambda^2 \end{pmatrix}. \tag{23}$$

This corresponds to the MX1 or MX3 mixing rules given in Ref. [8].

The fluctuation term of the free energy is given by

$$a_2 = \sum_{i=1}^{n} \sum_{j=1}^{n} x_{s,i} x_{s,j} a_2^{ij}. \tag{24}$$

Each of the terms a_2^{ij} are obtained with the local compressibility approximation (LCA) [33,34],

$$a_2^{ij} = \tfrac{1}{2}\, K^{\mathrm{HS}} \varepsilon_{ij} \rho_s \frac{\partial a_1^{ij}}{\partial \rho_s}, \tag{25}$$

where K^{HS} is the isothermal compressibility for a mixture of hard spheres, given by the Percus-Yevick expression [50],

$$K^{\mathrm{HS}} = \frac{\zeta_0 (1-\zeta_3)^4}{\zeta_0 (1-\zeta_3)^2 + 6\zeta_1\zeta_2(1-\zeta_3) + 9\zeta_2^3}. \tag{26}$$

For our particular system

$$a_2 = \tfrac{1}{2} K^{\mathrm{HS}} \varepsilon \rho_s \frac{\partial a_1}{\partial \rho_s}, \tag{27}$$

where K^{HS} is now the pure component expression given by

$$K^{\mathrm{HS}} = \frac{(1-\eta)^4}{(1-\eta)^2 + 6\eta(1-\eta) + 9\eta^2}. \tag{28}$$

The contribution to the free energy due to chain formation is given by

$$\frac{A^{\mathrm{chain}}}{NkT} = -\sum_{i=1}^{n} x_i (m_i - 1) \ln y_{ii}^{\mathrm{SW}}(\sigma_{ii}), \tag{29}$$

where $y_{ii}^{\mathrm{SW}}(\sigma_{ii}) = \exp(-\beta\varepsilon_{ii}) g_{ii}^{\mathrm{SW}}(\sigma_{ii})$ is the background correlation function, and $g_{ii}^{\mathrm{SW}}(\sigma_{ii})$ is the radial distribution function for the square-well system, both evaluated at contact. The term corresponding to the Boltzmann factor $\exp(-\beta\varepsilon_{ii})$ is not required in the phase equilibria calculations, so we can write

$$\frac{A^{\mathrm{chain}}}{NkT} = -\sum_{i=1}^{n} x_i (m_i - 1) \ln g_{ii}^{\mathrm{SW}}(\sigma_{ii}) = x_2 \ln g^{\mathrm{SW}}(\sigma). \tag{30}$$

We obtain the contact value of the radial distribution function for segments of species i and j from a first-order perturbation expansion

$$g_{ij}^{\mathrm{SW}}(\sigma_{ij}) = g_{ij}^{\mathrm{HS}}(\sigma_{ij}) + \beta\varepsilon_{ij} g_1(\sigma_{ij}), \tag{31}$$

where $g_1(\sigma_{ij})$ is obtained from a self-consistent calculation of the pressure using the Clausius virial theorem, as was explained in the original SAFT-VR paper [7]:

$$g_{ij}^{\mathrm{SW}}[\sigma_{ij};\zeta_3] = g_{ij}^{\mathrm{HS}}[\sigma_{ij};\zeta_3] + \beta\varepsilon_{ij}\left[g_{ij}^{\mathrm{HS}}[\sigma_{ij};\zeta_3^{\mathrm{eff}}] + (\lambda_{ij}^3 - 1) \times \left(\frac{\lambda_{ij}}{3} \frac{\partial g_{ij}^{\mathrm{HS}}[\sigma_{ij};\zeta_3^{\mathrm{eff}}]}{\partial \lambda_{ij}} - \rho_s \frac{\partial g_{ij}^{\mathrm{HS}}[\sigma_{ij};\zeta_3^{\mathrm{eff}}]}{\partial \rho_s} \right) \right]. \tag{32}$$

Since for our monomer-dimer mixture all of the square-well segments are the same size, the contact value of the square-well distribution function simplifies to

$$g^{\mathrm{SW}}[\sigma;\eta] = g^{\mathrm{HS}}[\sigma;\eta] + \beta\varepsilon\left[g^{\mathrm{HS}}[\sigma;\eta^{\mathrm{eff}}] + (\lambda^3 - 1) \times \frac{\partial g^{\mathrm{HS}}[\sigma;\eta^{\mathrm{eff}}]}{\partial \eta^{\mathrm{eff}}} \left(\frac{\lambda}{3} \frac{\partial \eta^{\mathrm{eff}}}{\partial \lambda} - \eta \frac{\partial \eta^{\mathrm{eff}}}{\partial \eta} \right) \right]. \tag{33}$$

This completes our description of the equation of state, as our system does not associate, $A^{\mathrm{assoc}} = 0$.

The pressure and chemical potential are required in order to determine the conditions of phase equilibria given by Eq. (1). The chemical potential μ_i of species i can be written in terms of the free energy:

$$\frac{\mu_i}{kT} = \left(\frac{\partial A/kT}{\partial N_i} \right)_{T,V,N_{j\neq i}}, \tag{34}$$

where N_i is the number of chain molecules of species i. The overall pressure P may be calculated through the compressibility factor Z as

$$Z = \frac{PV}{NkT} = \sum_{i=1}^{n} x_i \frac{\mu_i}{kT} - \frac{A}{NkT}, \tag{35}$$

where n is the total number of components in the mixture and $x_i = N_i/N$ is the mole fraction of component i. These functions are used in the numerical determination of the phase behavior of the mixture, using a simplex method [51].

IV. RESULTS

We examine the vapor-liquid equilibria of a binary square-well mixture of monomers (1) and dimers (2) with $\sigma = \sigma_{11} = \sigma_{12} = \sigma_{22}$, $\lambda = \lambda_{11} = \lambda_{12} = \lambda_{22} = 1.5$, and $\varepsilon = \varepsilon_{11} = \varepsilon_{12} = \varepsilon_{22}$. The reduced thermodynamic variables that we use are $\rho^* = N\sigma^3/V$ for the density, $T^* = kT/\varepsilon$ for the temperature, and $P^* = P\sigma^3/\varepsilon$ for the pressure. The mole fraction of monomers is $x_1 = N_1/N$ and of dimers is $x_2 = N_2/N$. The phase behavior of the mixture is summarized in Figs. 1 and 2, and the corresponding Gibbs ensemble data are reported in Tables I–VIII. As will become clear later, the mixture data can be used to estimate the vapor-liquid equilibria of each pure component fluid: the phase diagram of the monomer square-well system is shown in Fig. 3 and that of the square-well diatomic in Fig. 4, with the corresponding data given in Tables IX and X. A pressure-temperature projection of the full phase behavior, including the pure component data, is given in Fig. 5.

Pressure-composition (Px) constant temperature slices of the vapor-liquid phase diagram for the mixture are shown in

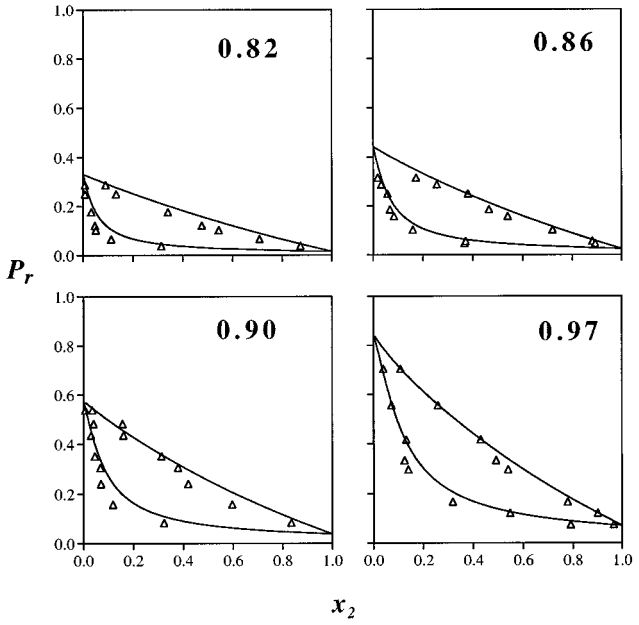

FIG. 1. Pressure-composition slices of the vapor-liquid coexistence for the square-well mixture of monomers (1) and dimers (2) with $\lambda=1.5$ for temperatures below the critical point of the pure monomer system. The reduced pressure $P_r=P^*/P^*_{c,1}$ is defined in terms of the critical point of the monomer, and x_2 is the mole fraction of dimers. The curves are labeled with their corresponding values of the reduced temperature $T_r=T^*/T^*_{c,1}$. The data points represent the results of the GEMC simulations for systems of $N=512$ particles, and the continuous curves correspond to the SAFT-VR prediction.

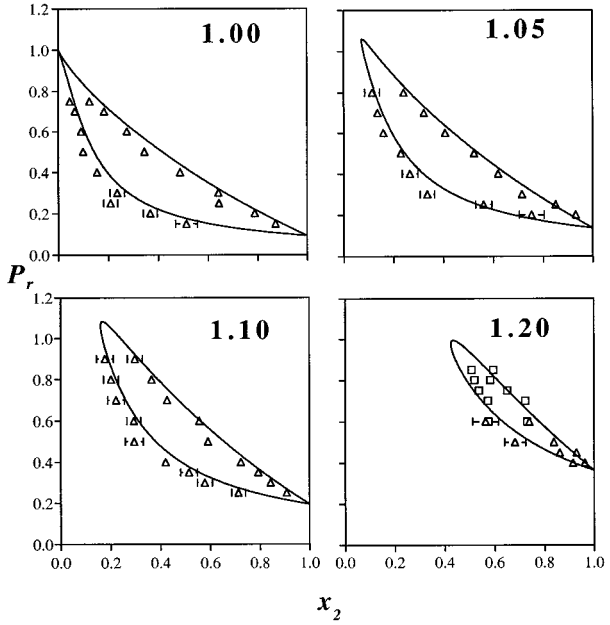

FIG. 2. Pressure-composition slices of the vapor-liquid coexistence for the square-well mixture of monomers (1) and dimers (2) with $\lambda=1.5$ for temperatures above the critical point of the pure monomer system. See Fig. 1 for details. The squares correspond to GEMC data for a system of $N=1728$ particles.

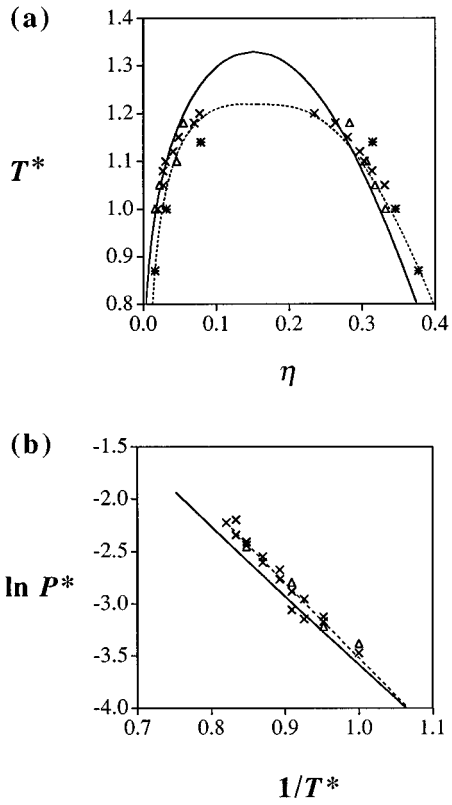

FIG. 3. (a) Vapor-liquid coexistence densities for the monomer square-well system with $\lambda=1.5$, where $T^*=kT/\varepsilon$ and $\eta=\pi\rho_s\sigma^3/6$ is the packing fraction. The triangles correspond to the results obtained by extrapolating the mixture GEMC data, the crosses correspond to the GEMC data of Ref. [40], and the asterisks to the molecular dynamics data of Ref. [39]. The continuous curve represents the SAFT-VR prediction and the dashed curve represents the Wegner expansion used in Ref. [40]. (b) Clausius-Clapeyron representation of the vapor pressures for the monomer fluid. The reduced pressure is defined as $P^*=P\sigma^3/\varepsilon$. The continuous line is the SAFT-VR prediction and the dashed line corresponds to the fit obtained in Ref. [40].

Figs. 1 and 2. The square-well dimer is the less volatile of the two components, and a slight negative deviation from Raoult's law can be detected. As the temperature is increased above the critical point of the pure monomer square-well fluid, vapor-liquid critical points are observed for the mixture. The GEMC simulation data are compared with the SAFT-VR predictions for a series of temperatures: four subcritical with respect to the pure monomer fluid, one at the estimated vapor-liquid critical temperature of the monomer ($T^*_{c,1}=1.22$ and $P^*_{c,1}=0.108$) [40], and three temperatures above the monomer critical point. Very good agreement between the theoretical predictions and the exact simulation data is observed for all temperatures studied. The comparisons have been made in terms of the reduced pressure and temperature with respect to the pure square-well monomer, $P_r=P^*/P^*_{c,1}$ and $T_r=T^*/T^*_{c,1}$. As has been mentioned in earlier work [7], the vapor-liquid critical point of the pure monomer square-well fluid is overestimated by the theory. By viewing the phase behavior of the monomer-dimer mixture in terms of reduced variables, we can focus on the ad-

TABLE I. Vapor-liquid coexistence data obtained from *NPT* Gibbs ensemble Monte Carlo simulations for a mixture of square-well monomers and dimers with a range $\lambda = 1.5$. The fixed variables during the simulation are the number of particles $N = 512$, the reduced pressure $P^* = P\sigma^3/\varepsilon$, and the reduced temperature $T^* = kT/\varepsilon = 1.00$. The packing fractions η, dimer mole fractions x_2, and the reduced energies per segment $E^* = E/\varepsilon N_s$ in the coexisting vapor and liquid phases are labeled v and l, respectively; the uncertainties correspond to one standard deviation.

P^*	η_v	η_l	$x_{2,v}$	$x_{2,l}$	E_v^*	E_l^*
0.004	0.003±0.0002	0.395±0.004	0.313±0.015	0.873±0.015	−0.10±0.03	−5.29±0.06
0.007	0.004±0.0004	0.389±0.004	0.112±0.020	0.708±0.017	−0.13±0.03	−5.27±0.07
0.011	0.006±0.001	0.383±0.004	0.051±0.019	0.544±0.012	−0.09±0.04	−5.26±0.07
0.013	0.008±0.001	0.379±0.004	0.047±0.016	0.476±0.012	−0.14±0.04	−5.25±0.07
0.019	0.012±0.001	0.376±0.006	0.032±0.012	0.339±0.017	−0.30±0.06	−5.29±0.08
0.027	0.015±0.002	0.374±0.008	0.007±0.009	0.132±0.007	−0.19±0.06	−5.44±0.11
0.031	0.021±0.002	0.366±0.008	0.007±0.006	0.090±0.005	−0.44±0.09	−5.36±0.12

TABLE II. Vapor-liquid coexistence data obtained from *NPT* Gibbs ensemble Monte Carlo simulations for a mixture of square-well monomers and dimers at a reduced temperature of $T^* = 1.05$. See Table I for details.

P^*	η_v	η_l	$x_{2,v}$	$x_{2,l}$	E_v^*	E_l^*
0.005	0.004±0.0003	0.388±0.004	0.366±0.020	0.892±0.015	−0.12±0.03	−5.17±0.06
0.006	0.004±0.0003	0.390±0.005	0.371±0.017	0.880±0.017	−0.15±0.03	−5.19±0.08
0.011	0.007±0.001	0.384±0.004	0.159±0.020	0.719±0.017	−0.20±0.04	−5.17±0.07
0.017	0.010±0.001	0.376±0.004	0.083±0.017	0.539±0.012	−0.23±0.05	−5.14±0.07
0.020	0.012±0.001	0.371±0.005	0.067±0.017	0.464±0.017	−0.30±0.05	−5.12±0.08
0.027	0.018±0.002	0.370±0.004	0.057±0.020	0.380±0.010	−0.47±0.10	−5.17±0.07
0.031	0.020±0.002	0.360±0.006	0.032±0.013	0.255±0.014	−0.47±0.08	−5.12±0.09
0.034	0.022±0.002	0.355±0.006	0.018±0.010	0.172±0.011	−0.54±0.09	−5.11±0.09

TABLE III. Vapor-liquid coexistence data obtained from *NPT* Gibbs ensemble Monte Carlo simulations for a mixture of square-well monomers and dimers at a reduced temperature of $T^* = 1.10$. See Table I for details.

P^*	η_v	η_l	$x_{2,v}$	$x_{2,l}$	E_v^*	E_l^*
0.009	0.006±0.001	0.377±0.004	0.322±0.023	0.834±0.017	−0.19±0.04	−5.00±0.08
0.017	0.010±0.001	0.365±0.005	0.117±0.021	0.596±0.015	−0.25±0.05	−4.94±0.07
0.026	0.016±0.002	0.355±0.006	0.069±0.017	0.419±0.013	−0.40±0.07	−4.91±0.09
0.033	0.022±0.002	0.359±0.006	0.067±0.015	0.378±0.013	−0.55±0.09	−4.99±0.09
0.038	0.021±0.002	0.357±0.006	0.045±0.018	0.312±0.010	−0.23±0.07	−5.00±0.09
0.047	0.038±0.008	0.345±0.007	0.030±0.018	0.160±0.009	−0.95±0.26	−4.96±0.11
0.052	0.050±0.009	0.342±0.006	0.040±0.013	0.156±0.008	−1.33±0.28	−4.93±0.09
0.058	0.051±0.007	0.341±0.013	0.007±0.007	0.035±0.003	−1.26±0.22	−5.02±0.18

TABLE IV. Vapor-liquid coexistence data obtained from *NPT* Gibbs ensemble Monte Carlo simulations for a mixture of square-well monomers and dimers at a reduced temperature of $T^* = 1.18$. See Table I for details.

P^*	η_v	η_l	$x_{2,v}$	$x_{2,l}$	E_v^*	E_l^*
0.008	0.007±0.001	0.368±0.005	0.790±0.015	0.966±0.008	−0.24±0.05	−4.80±0.07
0.013	0.011±0.001	0.370±0.005	0.547±0.017	0.900±0.015	−0.32±0.06	−4.89±0.08
0.018	0.012±0.001	0.361±0.005	0.317±0.024	0.778±0.017	−0.24±0.05	−4.77±0.08
0.032	0.019±0.002	0.368±0.006	0.139±0.022	0.539±0.017	−0.29±0.06	−4.71±0.09
0.036	0.022±0.002	0.348±0.007	0.124±0.018	0.491±0.016	−0.51±0.07	−4.66±0.10
0.045	0.032±0.004	0.343±0.007	0.131±0.019	0.429±0.018	−0.80±0.13	−4.70±0.11
0.060	0.047±0.005	0.328±0.010	0.072±0.013	0.258±0.020	−1.11±0.15	−4.61±0.14
0.076	0.077±0.012	0.306±0.010	0.039±0.014	0.108±0.008	−1.68±0.27	−4.45±0.14

TABLE V. Vapor-liquid coexistence data obtained from *NPT* Gibbs ensemble Monte Carlo simulations for a mixture of square-well monomers and dimers at a reduced temperature of $T^*=1.22$. See Table I for details.

P^*	η_v	η_l	$x_{2,v}$	$x_{2,l}$	E_v^*	E_l^*
0.016	0.013±0.001	0.357±0.006	0.513±0.044	0.827±0.018	−0.35±0.07	−4.67±0.08
0.022	0.015±0.002	0.354±0.006	0.368±0.028	0.788±0.017	−0.39±0.08	−4.65±0.08
0.027	0.016±0.002	0.336±0.007	0.209±0.028	0.644±0.018	−0.36±0.07	−4.48±0.09
0.032	0.022±0.002	0.345±0.007	0.236±0.029	0.642±0.022	−0.54±0.10	−4.59±0.10
0.043	0.029±0.004	0.333±0.008	0.155±0.023	0.488±0.023	−0.69±0.12	−4.51±0.11
0.054	0.036±0.005	0.316±0.010	0.099±0.022	0.345±0.021	−0.82±0.14	−4.38±0.13
0.065	0.052±0.007	0.314±0.009	0.091±0.019	0.274±0.016	−1.15±0.19	−4.40±0.13
0.076	0.067±0.018	0.299±0.010	0.066±0.022	0.183±0.010	−1.41±0.35	−4.26±0.13
0.081	0.071±0.010	0.285±0.014	0.046±0.018	0.125±0.010	−1.48±0.32	−4.14±0.17

TABLE VI. Vapor-liquid coexistence data obtained from *NPT* Gibbs ensemble Monte Carlo simulations for a mixture of square-well monomers and dimers at a reduced temperature of $T^*=1.28$. See Table I for details.

P^*	η_v	η_l	$x_{2,v}$	$x_{2,l}$	E_v^*	E_l^*
0.022	0.023±0.005	0.353±0.005	0.753±0.050	0.931±0.011	−0.65±0.19	−4.56±0.07
0.027	0.023±0.003	0.346±0.006	0.561±0.032	0.850±0.016	−0.62±0.11	−4.50±0.09
0.032	0.023±0.002	0.331±0.008	0.336±0.029	0.715±0.019	−0.55±0.10	−4.36±0.10
0.043	0.031±0.003	0.327±0.009	0.266±0.032	0.619±0.018	−0.71±0.12	−4.35±0.12
0.054	0.041±0.005	0.320±0.009	0.230±0.025	0.523±0.023	−0.94±0.14	−4.30±0.12
0.065	0.046±0.005	0.304±0.011	0.159±0.022	0.407±0.019	−1.00±0.13	−4.15±0.14
0.076	0.062±0.011	0.294±0.012	0.136±0.026	0.322±0.018	−1.30±0.24	−4.08±0.15
0.085	0.080±0.020	0.277±0.015	0.114±0.030	0.241±0.014	−1.60±0.36	−4.93±0.18

TABLE VII. Vapor-liquid coexistence data obtained from *NPT* Gibbs ensemble Monte Carlo simulations for a mixture of square-well monomers and dimers at a reduced temperature of $T^*=1.34$. See Table I for details.

P^*	η_v	η_l	$x_{2,v}$	$x_{2,l}$	E_v^*	E_l^*
0.027	0.025±0.003	0.329±0.008	0.713±0.028	0.907±0.012	−0.64±0.12	−4.23±0.10
0.032	0.028±0.003	0.325±0.008	0.577±0.030	0.842±0.016	−0.69±0.12	−4.21±0.10
0.038	0.033±0.005	0.324±0.007	0.514±0.034	0.793±0.017	−0.79±0.15	−4.21±0.10
0.043	0.035±0.004	0.316±0.009	0.420±0.027	0.723±0.020	−0.79±0.13	−4.13±0.11
0.054	0.040±0.006	0.296±0.010	0.294±0.036	0.590±0.018	−0.85±0.15	−3.95±0.12
0.065	0.051±0.006	0.299±0.012	0.292±0.028	0.555±0.020	−1.08±0.16	−3.99±0.14
0.076	0.066±0.011	0.280±0.015	0.221±0.033	0.426±0.019	−1.34±0.23	−3.83±0.17
0.086	0.077±0.012	0.266±0.018	0.201±0.030	0.364±0.018	−1.51±0.24	−3.71±0.20
0.097	0.088±0.025	0.235±0.039	0.177±0.034	0.297±0.003	−1.69±0.40	−3.43±0.41

TABLE VIII. Vapor-liquid coexistence data obtained from *NPT* Gibbs ensemble Monte Carlo simulations for a mixture of square-well monomers and dimers at a reduced temperature of $T^*=1.46$. See Table I for details. Results labeled with a † are obtained using $N=1728$ particles.

P^*	η_v	η_l	$x_{2,v}$	$x_{2,l}$	E_v^*	E_l^*
0.043	0.056±0.012	0.293±0.011	0.914±0.020	0.962±0.007	−1.17±0.26	−3.73±0.13
0.049	0.071±0.009	0.292±0.012	0.861±0.015	0.928±0.012	−1.47±0.17	−3.72±0.14
0.054	0.056±0.010	0.274±0.012	0.681±0.042	0.837±0.013	−1.12±0.22	−3.56±0.13
0.065	0.060±0.013	0.240±0.016	0.563±0.052	0.738±0.014	−1.17±0.26	−3.25±0.16
0.065†	0.070±0.004	0.250±0.013	0.575±0.015	0.731±0.013	−1.40±0.08	−3.35±0.13
0.076†	0.077±0.004	0.254±0.010	0.573±0.013	0.723±0.011	−1.51±0.08	−3.39±0.10
0.081†	0.101±0.012	0.235±0.019	0.537±0.024	0.651±0.015	−1.86±0.20	−3.23±0.18
0.086†	0.122±0.017	0.197±0.034	0.519±0.024	0.583±0.027	−2.13±0.22	−2.90±0.32
0.092†	0.113±0.011	0.212±0.024	0.508±0.020	0.595±0.017	−2.01±0.15	−3.04±0.22

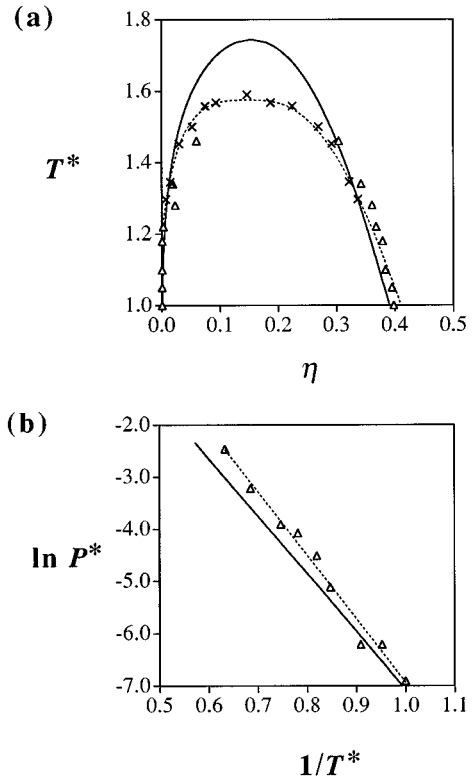

FIG. 4. (a) Vapor-liquid coexistence densities for the dimer square-well system with $\lambda = 1.5$ (see Fig. 3 for details). The crosses correspond to the Monte Carlo simulation data of Ref. [41]. The dashed curve is obtained by fitting a Wegner expansion to the simulation data of Ref. [41]. (b) Clausius-Clapeyron representation of the vapor pressures for the dimer fluid. The continuous line is the SAFT-VR prediction and the dashed line corresponds to a linear fit of the simulation data.

equacy of the theoretical prediction for the mixture, without clouding the comparison with the mediocre description of the pure component critical point.

Computer simulation data for the vapor-liquid phase behavior of the pure monomer system [39,40,5,6], and of the pure dimer system [41], have already been reported. The GEMC simulation data at each temperature are presented in Tables I–VIII. Our monomer-dimer data can be used to estimate the vapor-liquid coexistence of the individual components. We extrapolate the mixture Px data, using a linear

TABLE IX. Values of the reduced temperature $T^* = kT/\varepsilon$, the reduced vapor pressure $P^* = P\sigma^3/\varepsilon$, and the packing fractions η for the vapor-liquid coexistence of the pure square-well monomer fluid with a range $\lambda = 1.5$. The results are obtained by extrapolating the monomer-dimer mixture simulation data (see text for details). The vapor and liquid densities are denoted by v and l, respectively.

T^*	P^*	η_v	η_l
1.18	0.086	0.055	0.283
1.10	0.061	0.046	0.306
1.05	0.040	0.220	0.318
1.00	0.034	0.016	0.332

TABLE X. Values of the reduced temperature $T^* = kT/\varepsilon$, the reduced vapor pressure $P^* = P\sigma^3/\varepsilon$, and the packing fractions η for the vapor-liquid coexistence of the pure square-well dimer fluid with a range $\lambda = 1.5$. The results are obtained by extrapolating the monomer-dimer mixture simulation data (see text for details). The vapor and liquid densities are denoted by v and l, respectively.

T^*	P^*	η_v	η_l
1.46	0.040	0.060	0.304
1.34	0.020	0.019	0.342
1.28	0.017	0.023	0.361
1.22	0.011	0.003	0.368
1.18	0.006	$\leqslant 0.001$	0.379
1.10	0.002	$\leqslant 0.001$	0.384
1.05	0.002	$\leqslant 0.001$	0.395
1.00	0.001	$\leqslant 0.001$	0.398

Raoult's law dependence close to the $x_2 = 0$ and $x_2 = 1$ axes, to estimate values of the pure component vapor pressures. An extrapolation of the temperature-density data for the mixture is used to estimate the coexisting densities of the pure components. The large curvature of the data close to the pure monomer axes ($x_2 = 0$) made a linear extrapolation unsuit-

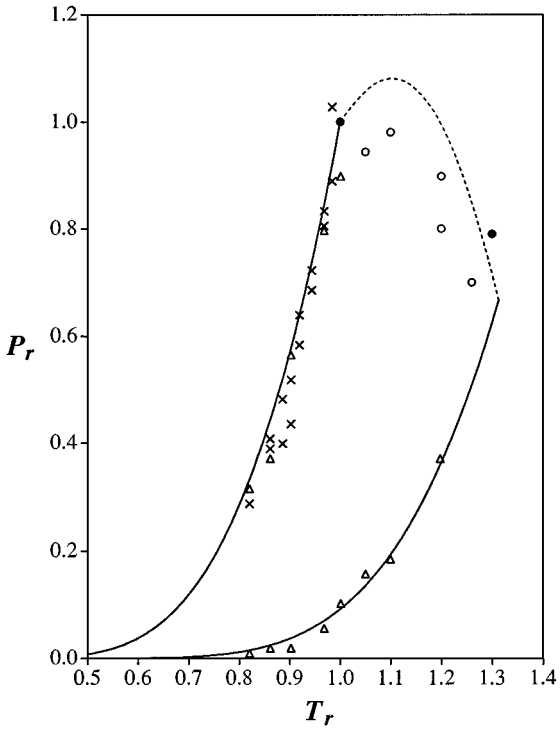

FIG. 5. Pressure-temperature projection for the binary mixture of square-well monomers and dimers. The reduced pressure $P_r = P^*/P^*_{c,1}$ and temperature $T_r = T^*/T^*_{c,1}$ are defined in terms of the critical point of the monomers. The triangles are the vapor pressures obtained by extrapolating the mixture GEMC data, the crosses are the GEMC data of Ref. [40], the circles correspond to the estimated vapor-liquid critical points, and the filled circles are the pure component critical points. The continuous and dashed curves represent the SAFT-VR prediction for the pure component vapor pressures and critical line, respectively.

able; the theory was used to guide the extrapolation in this case. The resulting estimates of the vapor-liquid equilibria for the pure component monomer and dimer systems are reported in Tables IX and X, respectively. The coexisting densities and vapor pressures (represented as Clausius-Clapeyron plots) are compared with the previous results in Figs. 3 and 4. It is gratifying to see that the extrapolation of the mixture data leads to values which are in close agreement with the previous data. As an added bonus, we can estimate the coexistence curve of the square-well dimer to much lower temperatures, and provide values for the vapor pressures which were not determined in the earlier work [41]. Also shown in these figures are the SAFT-VR predictions of the vapor-liquid phase equilibria. It has already been demonstrated that the SAFT-VR approach provides a good description of the phase envelope of the pure component monomer and dimer square-well systems [7], which is again apparent from an inspection of Figs. 3 and 4. In addition, we show a comparison of the SAFT-VR predictions for the vapor pressures of the pure components with the simulated values: SAFT-VR is again seen to provide a good description of the vapor pressures, although a slight underestimate is found. As was mentioned earlier, the SAFT-VR approach overpredicts the coexistence curve in the critical region, a feature which is common to all analytical equations of state [52]. This means that both the critical temperature and pressure occur at lower values than predicted by the SAFT-VR approach. The usual methodology for the determination of the critical parameters from Gibbs ensemble simulation data is from an appropriate critical expansion (e.g., see Refs. [40,4]). The coexistence curves obtained from a fit to the data using a Wegner expansion with a fixed critical exponent of $\beta=0.325$, and the fit of the vapor-pressure curves using a Clausius-Clapeyron plot, are also shown in the figures for both the monomers and dimers (see Ref. [40] for details). The corresponding estimates for the critical parameters are $T^*_{c,1}=1.22$, $P^*_{c,1}=0.108$, and $\eta_{c,1}=0.157$ for the monomer [40], and $T^*_{c,2}=1.58$, $P^*_{c,1}=0.085$, and $\eta_{c,1}=0.147$ for the dimer; the latter are in good agreement with the estimates of $T^*_{c,2}=1.59$ and $\eta_{c,2}=0.14$ by Yethiraj and Hall [41], but $P^*_{c,2}=0.085$ is a new estimate for the critical pressure.

The critical points in mixtures can also be obtained by analyzing the simulation data in terms of a Wegner expansion (see Ref. [4] for details). In our case an expansion including the first extension to scaling term was used to estimate the critical points at constant temperature; a simple extrapolation was made for the constant pressure slices. Due to the limited amount of simulation data close to the critical region, only rough estimates of the vapor-liquid critical points could be made. The resulting vapor-liquid critical line of the monomer-dimer mixture is presented as a pressure-temperature PT projection in Fig. 5, together with the vapor-pressure curves of the two pure components. The vapor-liquid critical line is continuous and extends from the critical point of the monomer to that of the dimer. There is no liquid-liquid immiscibility in this system due to the similarity in the attractive interactions. This type of vapor-liquid equilibria corresponds to type I in the classification of Scott and van Konynenburg [53,54]. The vapor-liquid critical line of our monomer-dimer mixture also exhibits a maximum in pressure, a feature which is reproduced by the SAFT-VR predictions. As was mentioned earlier, the SAFT-VR theory is seen to provide an excellent description of the vapor-pressure curves for both the monomers and dimers. The critical points estimated from the GEMC coexistence data are seen to deviate from the predicted critical line, although a large amount of scatter is evident.

V. CONCLUSIONS

In our monomer-dimer square-well mixture all of the segment-segment interactions are the same. Accordingly, the phase behavior exhibited by the mixture is a consequence of the difference in length of the dimer and monomer molecules. The pressure-composition slices of the phase diagram obtained using the Gibbs ensemble technique indicate that there is a small negative deviation from Raoult's law; the nonideality can be attributed entirely to the difference in chain length in this case. As an interesting aside we note that it is possible to obtain reasonable estimates of the pure component phase equilibria by extrapolating the mixture data. Due to its simplicity, the monomer-dimer mixture offers an ideal testing ground for equations of state for chain molecules. The statistical associating fluid theory for potentials of variable range (SAFT-VR) is one such theory. The phase equilibria of the monomer-dimer mixture predicted with the SAFT-VR equation of state compares favorably with the exact simulation data. This study represents the first test of the adequacy of the SAFT-VR approach to model mixtures comprising chain molecules.

ACKNOWLEDGMENTS

L.A.D. thanks the Engineering and Physical Sciences Research Council (EPSRC) and BP for financial support, and A.G.V. thanks the EPSRC and ICI for support. We also acknowledge support from the European Commission (Grant No. CI1*-CT94-0132), the Royal Society, and the Computational and ROPA Initiatives of the EPSRC.

[1] A. Z. Panagiotopoulos, Mol. Phys. **61**, 813 (1987).
[2] A. Z. Panagiotopoulos, N. Quirke, M. R. Stapleton, and D. J. Tildesley, Mol. Phys. **63**, 527 (1988).
[3] A. Z. Panagiotopoulos, Mol. Simul. **9**, 1 (1992).
[4] D. G. Green, G. Jackson, E. de Miguel, and L. F. Rull, J. Chem. Phys. **101**, 3190 (1994).
[5] J. R. Recht and A. Z. Panagiotopoulos, Mol. Phys. **80**, 843 (1993).
[6] E. de Miguel, Phys. Rev. E **55**, 1347 (1997).
[7] A. Gil-Villegas, A. Galindo, P. J. Whitehead, S. J. Mills, G. Jackson, and A. N. Burgess, J. Chem. Phys. **106**, 4168 (1997).
[8] A. Galindo, L. A. Davies, A. Gil-Villegas, and G. Jackson, Mol. Phys. (to be published).
[9] W. G. Chapman, K. E. Gubbins, G. Jackson, and M. Radosz, Fluid Phase Equilibria **52**, 31 (1989).
[10] W. G. Chapman, K. E. Gubbins, G. Jackson, and M. Radosz,

Ind. Eng. Chem. Res. **29**, 1709 (1990).
[11] M. S. Wertheim, J. Stat. Phys. **35**, 19 (1984).
[12] M. S. Wertheim, J. Stat. Phys. **35**, 35 (1984).
[13] M. S. Wertheim, J. Stat. Phys. **42**, 459 (1986).
[14] M. S. Wertheim, J. Stat. Phys. **42**, 477 (1986).
[15] M. S. Wertheim, J. Chem. Phys. **85**, 2929 (1986).
[16] M. S. Wertheim, J. Chem. Phys. **87**, 7323 (1987).
[17] W. G. Chapman, J. Chem. Phys. **93**, 4299 (1990).
[18] D. Ghonasgi and W. G. Chapman, Mol. Phys. **80**, 161 (1993).
[19] J. K. Johnson, E. A. Müller, and K. E. Gubbins, J. Phys. Chem. **98**, 6413 (1994).
[20] M. Banaszak, Y. C. Chiew, R. Olenick, and M. Radosz, J. Chem. Phys. **100**, 3803 (1994).
[21] M. Banaszak, Y. C. Chiew, and M. Radosz, Phys. Rev. E **48**, 3760 (1993).
[22] D. Ghonasgi and W. G. Chapman, J. Chem. Phys. **100**, 6633 (1994).
[23] F. W. Tavares, J. Chang, and S. I. Sandler, Mol. Phys. **86**, 1451 (1995).
[24] R. Sear and G. Jackson, Mol. Phys. **82**, 1033 (1994).
[25] D. Ghonasgi, V. Perez, and W. G. Chapman, J. Chem. Phys. **101**, 6880 (1994).
[26] D. Ghonasgi and W. G. Chapman, J. Chem. Phys. **102**, 2585 (1995).
[27] R. P. Sear and G. Jackson, Phys. Rev. E **50**, 386 (1994).
[28] R. P. Sear and G. Jackson, Mol. Phys. **87**, 517 (1996).
[29] R. P. Sear and G. Jackson, J. Chem. Phys. **105**, 1113 (1996).
[30] R. P. Sear and G. Jackson, Mol. Phys. **82**, 473 (1994).
[31] S. C. McGrother, R. P. Sear, and G. Jackson, J. Chem. Phys. **106**, 7315 (1997).
[32] L. A. Davies, A. Gil-Villegas, and G. Jackson, Int. J. Thermophys. (to be published).
[33] J. A. Barker and D. Henderson, J. Chem. Phys. **47**, 2856 (1967).
[34] J. A. Barker and D. Henderson, J. Chem. Phys. **47**, 4714 (1967).
[35] J. A. Barker and D. Henderson, Rev. Mod. Phys. **48**, 587 (1976).
[36] K. E. Gubbins, Mol. Simul. **2**, 223 (1989).
[37] A. L. Archer and G. Jackson, Mol. Phys. **73**, 881 (1991).
[38] L. F. Rull, G. Jackson, and B. Smit, Mol. Phys. **85**, 435 (1995).
[39] G. A. Chapela, S. E. Martínez-Casas, and C. Varea, J. Chem. Phys. **86**, 5683 (1987).
[40] L. Vega, E. de Miguel, L. F. Rull, G. Jackson, and I. A. McLure, J. Chem. Phys. **96**, 2296 (1992).
[41] A. Yethiraj and C. K. Hall, Mol. Phys. **72**, 619 (1991).
[42] W. W. Wood, J. Chem. Phys. **48**, 415 (1968).
[43] M. P. Allen and D. J. Tildesley, *Computer Simulations of Liquids* (Clarendon Press, Oxford, 1987).
[44] B. Widom, J. Chem. Phys. **39**, 2808 (1963).
[45] B. Smit and D. Frenkel, Mol. Phys. **68**, 951 (1989).
[46] L. L. Lee, *Molecular Thermodynamics of Nonideal Fluids* (Butterworth Scientific, London, 1988).
[47] T. Boublík, J. Chem. Phys. **53**, 471 (1970).
[48] G. A. Mansoori, N. F. Carnahan, K. E. Starling, and T. W. Leland, J. Chem. Phys. **54**, 1523 (1971).
[49] N. F. Carnahan and K. E. Starling, J. Chem. Phys. **51**, 635 (1969).
[50] T. M. Reed and K. E. Gubbins, *Applied Statistical Mechanics* (McGraw-Hill, New York, 1973).
[51] W. H. Press, B. P. Flannery, S. A. Teukolsky, and W. T. Vetterling, *Numerical Recipes*, 2nd ed. (Cambridge University Press, Cambridge, 1992).
[52] H. E. Stanley, *Introduction to Phase Transitions and Critical Phenomena* (Oxford University Press, Oxford, 1987).
[53] P. H. van Konynenburg and R. L. Scott, Philos. Trans. R. Soc. London, Ser. A **298**, 495 (1980).
[54] J. S. Rowlinson and F. L. Swinton, *Liquids and Liquid Mixtures*, 3rd ed. (Butterworth Scientific, London, 1982).